ASIAN JOURNAL OF CIVIL ENGINEERING (BHRC) VOL. 17, NO. 7(2016)
PAGES 937-957

INELASTIC POST-BUCKLING ANALYSIS OF SPACE TRUSSES USING FIXED INCEREMENTAL DISPLACEMENT METHOD

S. Rostami, S. Shojaee* and E. Izadpanah
Department of Civil Engineering, Shahid Bahonar University of Kerman, Kerman, Iran

Received: 2 January 2016; **Accepted:** 26 March 2016

ABSTRACT

This paper presents a novel scheme for large deformation analysis of space truss structures, including both geometric and material nonlinearities, using a predictor-corrector procedure, titled as fixed incremental displacement (FID) method. The nonlinear equilibrium equations are solved using an incremental-iterative method based on the displacement control scheme, as, by employing a specified displacement, the corresponding load will be obtained. In the present method, the ratio of the size of increment displacement vector to that of total displacement is assumed to be constant at the beginning of each increment. The geometric nonlinearity is considered based on an updated Lagrangian formulation, while the material nonlinearity is accounted for by tracing a complete stress-strain relationship. A computer program based on the algorithm is developed for analysis of space structures with complex behaviors, including snap-through buckling, snap-back, unloading and inelastic post-buckling analysis. This algorithm can accurately trace the equilibrium path of nonlinear problems. To demonstrate the efficiency and accuracy of the method developed here, some well-known trusses are investigated and analyzed using the aforementioned algorithm and the results are compared with those of cylindrical arc-length method.

Keywords: Nonlinear; inelastic analysis; FID method; space truss; snap-through; post buckling.

1. INTRODUCTION

Nowadays, non-linear analysis of structures has become an attractive matter and appears necessary for most structural engineering applications, whereas tendency for more accurate structural analysis has increased by many engineers. For only geometric non-linearity, incremental procedures were originally adopted by Turner *et al.* [1] and Argyris [2] using the geometric stiffness matrix in conjunction with an updating of coordinates and, possibly,

*E-mail address of the corresponding author: saeed.shojaee@uk.ac.ir (S. Shojaee)

an initial displacement matrix. A similar approach was adopted with material non-linearity [3,4]. In particular, for plasticity, the structural tangent stiffness matrix (relating increment of load to increments of displacement) incorporated a tangential modular matrix which related the increments of stress to the increments of strain [4,5].

The non-linear behavior of trusses has been investigated extensively by utilizing various member models and non-linear analysis methods as presented by Papadrakakis [6], Smith [7], Murtha-Smith [8], Hill et al. [9], de Freitas and Ribei [10], among others. Murtha-Smith [11] and Blandford [12] reviewed these models. Truss structures realistic behavior represented by many researchers. Hill et al. [9]proposed a truss model behavior based on the experimental equations of stress-strain relationship. Their model traces the inelastic post-buckling response of truss members in the post-buckling range using appropriate constitutive equations. The capabilities of the Hill et al.'s model are extended by Blandford [13,14] and Ramesh and Krishnamoorthy [15] using the arc-length method and dynamic relaxation method respectively.

The most complete nonlinear analysis of truss structures is a kind of analysis in which bothgeometric and material nonlinearity have considered duringthe analysis process. Jagannathan et al. [16] have considered a total Lagrange formulation with elastic material properties on the geometric nonlinear analysis of space trusses using Green-Lagrange representation of the axial strain. Papadrakakis [6] has used the dynamic relaxation method for the large displacement analysis of trusses. Blandford [13] has considered static analysis of space truss structures including inelastic material and large deformation geometric nonlinearities. Nonlinear analysis problem, formulated as an application of minimum potential energy principle, is obviously an optimization problem, have been presented by Toklu [17]. Saffari and Mansouri [18] proposed two-point method for non-linear analysis of space truss structures. Also a new approach for nonlinear analysis of structures, using cubic spline function, introduced by Saffari et al. [19] accelerates the convergence rate.

The space trusses have highly nonlinear behavior regarding the number of degrees of freedom and the level of load applied. Among the nonlinear analysis methods, simple iterative and incremental methods are weak in passing the limit points of snap-through or snap-back of the trusses. In fact, they may fail in passing the limit points of load and displacement. The concept of combining incremental (predictor) and iterative (corrector) methods was introduced by Brebbia and Connor [20] and Murray and Wilson [21] who thereby adopted a form of 'continuation method'. Among the methods for solving the nonlinear system of equations, the incremental iterative Newton-Raphson method is used much more, Oden [22]. The Newton-Raphson method is one powerful approach to evaluate the response of a structure to a set of successive loads. Amodified Newton-Raphson procedure was also recommended by Oden [23], and Zienkiewicz [4]. In contrast to the full Newton-Raphson method, the stiffness matrix would not be continuously updated. However, this method diverges when the solution is close to limit points so is not able to present the real behavior of the structure. As the load level is constant in the method of load increments, passing the limit points is not possible. Also, if there are serious changes in the load-displacement path, the number of iterations for convergence will be increased and so the method will be time consuming and expensive [24].

A complete investigation of the large displacement inelastic behavior of structures

requires tracing the equilibrium path and identifying the critical points. To achieve this, several techniques and methods have been presented in the literature. In the structures with complex behavior the load-displacement curve is a combination of softening and hardening states with limit points. A limit point refers to the turning point for the equilibrium path of a structure, which can be further considered as the transition point from stable to unstable equilibrium states or vice versa. In analysis of such structures, the simple incremental iterative methods unable to pass this limit points. The simple incremental iterative methods couldn't trace the equilibrium path after the limit points. For resolving such disadvantages, advanced analysis methods have been developed [25]. To overcome these limitation, many solution algorithms or combined methods have been presented and various methods for enhancement of the analysis speed have been presented by researchers. Eriksson [26] introduced Several path-following procedures, based on analytical elastic stability theory, for geometrically nonlinear structural analysis. Kwasniewski [27] suggested the complete equilibrium paths for several trusses. Riks [28,29] proposed the arc-length method, and Crisfield [30] also proposed several different versions of the arc-length method by updating constraint equations. An algorithm, known as the modified normal flow algorithm, for geometrically nonlinear analysis of space trusses, especially for passing the equilibrium path, was proposed by Saffari *et al*. [31]. Generalized displacement control (GDC) method for large-deflection elastic and inelastic post-buckling analysis of space truss structures presented by Thai and Kim [32]. In a novel work Saffari *et al*. [33] introduce an efficient numerical method in second-order inelastic analysis of space trusses. In this paper, the Newton-Raphson method is combined with three different algorithms includes the generalized minimum residual, the least squares, and the biconjugate gradient. Of these algorithms, the most effective at reducing the number of iterations and the time required is identified.

Using fixed incremental displacement algorithm, this paper, proposed a novel method that has a possibility of passing the limit points in the case of highly nonlinear behavior state. In the fixed incremental displacement algorithm the nonlinear equilibrium equations are solved using an incremental-iterative method, based on the displacement control scheme, as, by employing a specified displacement, the corresponding load will be obtained. In the present method, the ratio of the size of increment displacement vector to that of total displacement is assumed to be constant at the beginning of each increment.

This paper is organized as follows. In the next section, we will have a brief review of nonlinear analysis of trusses, including both geometric and material nonlinearity. Section 3 is allocated to implementation of FID method for nonlinear analysis. In section 4, the validity of the proposed method is illustrated with some examples.

2. NONLINEAR ANALYSIS OF SPACE TRUSSES

Nonlinear analysis becomes necessary when the stiffness of the part changes under its operating conditions. If changes in stiffness come only from changes in shape, nonlinear behavior is defined as geometric nonlinearity. In fact, in this case, large displacement and small strain occur. If changes in stiffness come from changes in stress-strain relation,

nonlinear behavior is defined as material nonlinearity. The accurate case is that both material and geometric effects are considered in structural analysis.

Large displacement inelastic analysis of space trusses, including both geometric and material nonlinearities is discussed below. A number of models have been developed to predict the nonlinear behavior of space trusses. The accuracy of the stress-strain relationship used, affect the inelastic post-buckling response of truss structures. In the present study, a relatively simple stress-strain relationship, proposed by Hill et al. [9], is adopted to predict the inelastic post-buckling behavior of truss members. The method of analysis used in this paper is based on the work carried out by Kassimali and Bidhendi [34].

Fig. 1 shows a typical prismatic member of a space truss. Let F_1 to F_6 denote member end forces referring to a general global system as shown in Fig. 1(a), and V_1 to V_6 are the corresponding end displacements. For this truss member in its initial configuration, the global nodal coordinates are defined as (X_1, Y_1, Z_1) and (X_2, Y_2, Z_2), for node 1 and 2, respectively. For the truss member in its current configuration (deformed shape), the global nodal coordinates are $(X_1+V_1, Y_1+V_2, Z_1+V_3)$ for node 1 and $(X_1+V_1, Y_1+V_2, Z_1+V_3)$ for node 2.

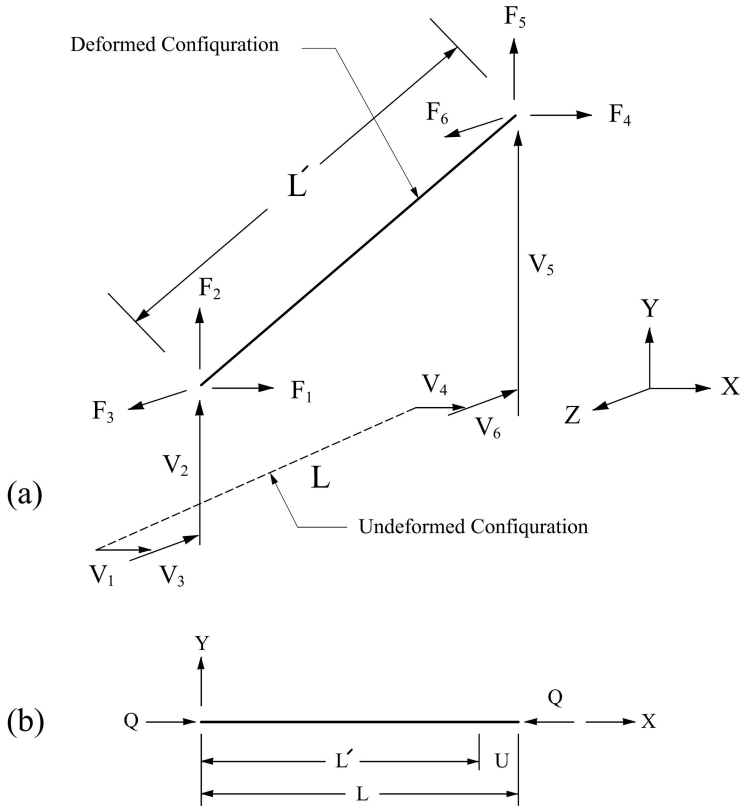

Figure 1. Force and displacement in global and local coordinates: (a) the force and deformation of member in general system; (b) the member in the local coordinate

Fig. 1(b) shows a typical prismatic member of a space truss in the local coordinate. The relationship between member end forces in global and local coordinates is given by

$$\{F\} = Q\{B\} \tag{1}$$

In which Q is the member axial force in local coordinates and $\{B\}$ is the transformation vector, which can be expressed as follows

$$\{B\} = \{l \quad m \quad n \quad -l \quad -m \quad -n\}^T \tag{2}$$

In which l, m, n are the direction cosines of the member axis in the deformed configuration (line connecting element nodal points) and L' is the member length in the deformed configuration. The member axial deformation, u, in local coordinates can be expressed in terms of initial length, L, and deformed length, L', as

$$u = L - L' \tag{3}$$

The axial force in the truss member is $Q = A\sigma$ as A is cross sectional area and σ defined in the cases below.

For tensile members:

$$\sigma = E\varepsilon, \quad \varepsilon < \varepsilon_y \tag{4a}$$

$$\sigma = \sigma_y, \quad \varepsilon \geq \varepsilon_y \tag{4b}$$

For compressive members:

$$\sigma = E\varepsilon, \quad |\varepsilon| < |\varepsilon_{cr}| \tag{5a}$$

$$\sigma = \sigma_l + (\sigma_{cr} - \sigma_l)\exp\left[\left(\bar{X}_1 + \bar{X}_2\sqrt{\varepsilon'}\right)\varepsilon'\right], \quad |\varepsilon| \geq |\varepsilon_{cr}| \tag{5b}$$

where ε_y and σ_y are the yield strain and corresponding yield stress, respectively; $\bar{X}_1$ and $\bar{X}_2$ are the constants depending on slenderness ratio (L/r) of the compressive members; $\sigma_l = r\sigma_{cr}$ is the asymptotic lower stress limit; $\varepsilon' = |\varepsilon| - \varepsilon_{cr}$ is the axial strain measured from the beginning of the inelastic post-buckling range, as shown in Fig. 2; $\sigma_{cr} = \pi^2 EI / AL^2$ and $\varepsilon_{cr} = \sigma_{cr} / E$ are the Euler critical buckling stress and corresponding critical buckling strain, respectively. In which E is the elastic modulus of material; I, A and L are the weak axis moment of inertia, area, and length of truss element, respectively [32]. The term ε inEqs. (4) and (5) describes strain that can be defined in terms of engineering, logarithmic, Green

or Almansi strain [24]. In this paper we used engineering strain, so $\varepsilon = \left(L'/L\right) - 1$.

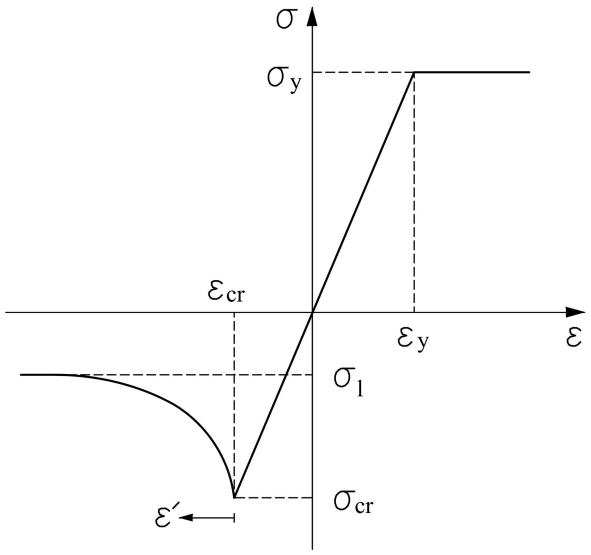

Figure 2. Assumed stress-strain curve for loading path

The incremental form of the equilibrium equation for the truss element, subjected to external forces, $\{P\}$, can be derived as

$$\{f(u)\} = \{P\} \tag{6}$$

In which $\{f\}$ is the resultant internal forces, and $\{u\}$ is the generalized coordinates consisting of the translation of end joints. The member force deformation relationships denote that $\{f\}$ is a highly nonlinear function of $\{u\}$. The incremental form of the Eq. (6) can be rewritten as follows

$$[\tau]\{\Delta u\} = \{\Delta P\} \tag{7}$$

where $[\tau]$ is the system tangent stiffness matrix obtained from assembling the tangential stiffness matrixes of the members, $\{\Delta u\}$ is the displacement increment vector, and $\{\Delta P\}$ is load increments. The tangential stiffness matrix of the member, $[T]$, can be expressed by

$$[T] = \left(\frac{A\bar{E}}{L}\right)\{B\}\{B\}^T + Q[g] \tag{8}$$

where [g] is geometric matrix that can be found in Tezcan [35]; and $\bar{E}$ is the same as E as for the elastic case and elasto-plastic tangent modulus after yield stress. When a member is in the compression state and $|\varepsilon| \geq |\varepsilon_{cr}|$, for the inelastic case, it is equal to the tangent modulus

$$\bar{E} = -(\sigma_{cr} - \sigma_1)\exp\left[\left(\bar{X}_1 + \bar{X}_2\sqrt{\varepsilon'}\right)\varepsilon'\right].\left(\bar{X}_1 + \frac{3}{2}\bar{X}_2\sqrt{\varepsilon'}\right) \tag{9}$$

Unlike the compressive loading path, which is the same for all members with the same slenderness ratio, compressive unloading paths are dependent on the state of stress in each member at the instant of loading [6]. A member unloading from the inelastic post-buckling range $\left(|\varepsilon| \geq |\varepsilon_{cr}|\right)$, as shown in Fig. 3, will follow a much more complex unloading curve. Since it is difficult to develop a constitutive equation adequate for modeling stress reversal in buckled members, a simplified assumption has been adopted. The unloading path of buckled members in the inelastic post-buckling range, as shown in Fig. 3, is assumed as a straight line from the stress σ_r and strain ε_r, at stress reversal, to a stress and strain corresponding to one-half of the material yield stress σ_y. When the loading path reaches point*A*, member behavior follows relations in Eq. (4).

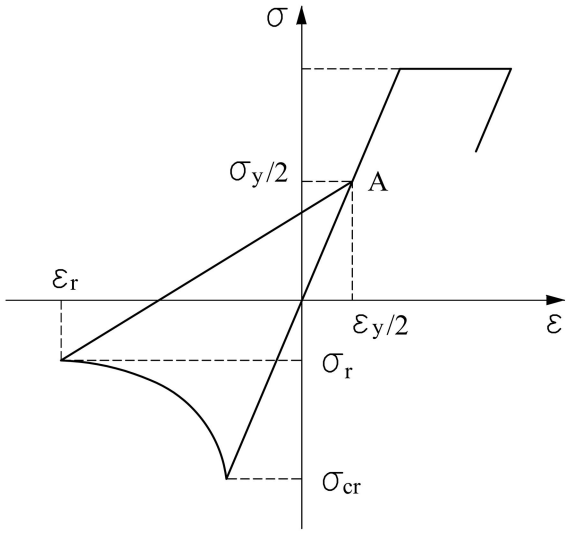

Figure 3. Assumed stress-strain curve for unloading path

3. FID METHOD

There are many methods for nonlinear analysis of structures in the literature. Among them, the line search technique is widely used within mathematical programming. There are a wide

range of procedures developed within this field which are extremely relevant to nonlinear analysis. The main process of the method proposed herein is also based on the line search technique. In the following section this proposed method has been described.

3.1 Main concepts

The equilibrium equation of nonlinear system can be written as

$$R\left(u,\lambda\right)=F_{\text{int}}(u)-\lambda F_{ext} \tag{10}$$

where F_{int} are the internal forces which are functions of displacement, u, the vector F_{ext} is a fixed external loading vector and the scalar $\lambda\ \left(0\le\lambda\le1\right)$ is a load-level parameter that multiplies F_{ext}.

The method proposed in this paper is based on displacement control, as by employing a specified displacement, corresponding load will be obtained. In the present method, the ratio of the size of increment displacement vector to the size of total displacement is assumed to be equal to a parameter entitled as *FID* that is constant at the beginning of each increment. So,

$$FID_i^n=\frac{\left|\delta d_i^n\right|}{\left|d_i^n\right|}. \tag{11}$$

In the above equation d_i^n and δd_i^n are total displacement vector and increment displacement vector pertinent to the i^{th} iteration of the n^{th} load increment, respectively. So once the displacement increment vector, δd_i^n, is determined, the total displacement vector of structure, d_i^n, at the end of the i^{th} iteration can be accumulated as $d_i^n=d_{i-1}^n+\delta d_i^n$. The term FID_i^n (Fixed Incremental Displacement) is a constant parameter, $0<FID_i^n\le1$, the value of which can be fixed or variable during loading of structure. In this paper, a constant value is considered for this parameter at the beginning of each increment (load step), as this value declines gradually in each iteration until convergence is achieved. δd_i^n is defined as

$$\delta d_i^n=-\left(K_i^n\right)^{-1}R_i^n=-\left(K_i^n\right)^{-1}\left(\left(F_{\text{int}}\right)_i^n-\lambda_i^n F_{ext}\right) \tag{12}$$

in the above equation, K_i^n and R_i^n are tangent stiffness matrix and unbalanced force vector in the i^{th} iteration of the n^{th} load increment, respectively. $\left(F_{\text{int}}\right)_i^n$ and F_{ext} are the internal force vector in the current step and vector of loading pattern (Fixed external load), respectively. λ_i^n is load coefficient considered as unknown. Eq. (12) can be broken into the following equations.

$$\delta d_i^n = \delta \bar{d}_i^n + \lambda_i^n \delta \hat{d}_i^n \tag{13}$$

$$\delta \bar{d}_i^n = -\left(K_i^n\right)^{-1} \left(F_{\text{int}}\right)_i^n \tag{14}$$

$$\delta \hat{d}_i^n = \left(K_i^n\right)^{-1} F_{ext} \tag{15}$$

By replacing the denominator in Eq. (11) with $d_{i-1}^n + \delta d_i^n$ and using Eq. (13), after some algebraic operation and simplification, a quadratic equation is achieved in terms of λ_i^n as

$$a_1 \left(\lambda_i^n\right)^2 + a_2 \lambda_i^n + a_3 = 0 \tag{16}$$

where

$$a_1 = \left(\left(FID_i^n\right)^2 - 1\right)\left(\delta \hat{d}_i^n . \delta \hat{d}_i^n\right) \tag{17a}$$

$$a_2 = 2\left(\left(\left(FID_i^n\right)^2 - 1\right)\left(\delta \bar{d}_i^n . \delta \hat{d}_i^n\right) + \left(FID_i^n\right)^2 \left(d_{i-1}^n . \delta \hat{d}_i^n\right)\right) \tag{17b}$$

$$a_3 = \left(\left(FID_i^n\right)^2 - 1\right)\left(\delta \bar{d}_i^n . \delta \bar{d}_i^n\right) + \left(FID_i^n\right)^2 \left(2 d_{i-1}^n . \delta \bar{d}_i^n + d_{i-1}^n . d_{i-1}^n\right) \tag{17c}$$

In Eqs. (17a) to (17c), the sign "." represents the inner product of two vectors. The quadratic Eq. (16) has two roots, λ_1 and λ_2. The acceptance criteria for these answers will be discussed in the next section.

3.2 Acceptance criteria of λ

In order to select appropriate λ, one must firstly address the issue of finding appropriate root of Eq. (16). Since vectors δd_i^n and δd_{i-1}^n should not be in opposite directions, Eq. (18) must be satisfied.

$$\left(\delta d_i^n . \delta d_{i-1}^n\right) > 0 \tag{18}$$

Substituting Eq. (13) in Eq. (18) will give

$$\left(\delta \bar{d}_i^n . \delta d_{i-1}^n\right) + \lambda_i^n \left(\delta \hat{d}_i^n . \delta d_{i-1}^n\right) > 0 \tag{19}$$

Depending on the sign of $(\delta \hat{d}_i^n . \delta d_{i-1}^n)$ the above inequality is rewritten into the form below

$$\begin{cases} \lambda_i^n > \lambda_c & , \quad (\delta\hat{d}_i^n.\delta d_{i-1}^n) > 0 \\ \lambda_i^n < \lambda_c & , \quad (\delta\hat{d}_i^n.\delta d_{i-1}^n) < 0 \end{cases} \quad , \quad \lambda_c = -\frac{(\delta\bar{d}_i^n.\delta d_{i-1}^n)}{(\delta\hat{d}_i^n.\delta d_{i-1}^n)} \tag{20}$$

From the results obtained by Eq. (16), one that is acceptable when it satisfies Eq. (20). Acceptable value λ_i^n can be obtained using the following equation:

$$\begin{cases} \lambda_i^n = \max(\lambda_1, \lambda_2, \lambda_c), & (\delta\hat{d}_i^n.\delta d_{i-1}^n) > 0 \\ \lambda_i^n = \min(\lambda_1, \lambda_2, \lambda_c), & (\delta\hat{d}_i^n.\delta d_{i-1}^n) < 0 \end{cases} \tag{21}$$

3.3 Acceptance criteria of FID parameter

As it is clear from Eqs. (17), coefficients of quadratic equation (i.e Eq. (16)) depend on FID_i^n parameter. In order for the values obtained for λ_i^n to be real, it is necessary that the following equation are satisfied.

$$a_2{}^2 - 4a_1a_3 \geq 0 \tag{22}$$

Substituting Eq. (17) into Eq. (22) we will have

$$b_1\left(FID_i^n\right)^4 + b_2\left(FID_i^n\right)^2 + b_3 \geq 0 \tag{23}$$

where constant coefficients are defined as follows

$$b_1 = \left(\left(\delta\bar{d}_i^n.\delta\hat{d}_i^n\right) + \left(d_{i-1}^n.\delta\hat{d}_i^n\right)\right)^2 - \left(\delta\hat{d}_i^n.\delta\hat{d}_i^n\right)\left(\left(\delta\bar{d}_i^n.\delta\bar{d}_i^n\right) + \left(d_{i-1}^n.d_{i-1}^n\right) + 2\left(d_{i-1}^n.\delta\bar{d}_i^n\right)\right) \tag{24a}$$

$$\begin{aligned} b_2 = {} & 2\left(\delta\hat{d}_i^n.\delta\hat{d}_i^n\right)\left(\left(\delta\bar{d}_i^n.\delta\bar{d}_i^n\right) + \left(d_{i-1}^n.\delta\bar{d}_i^n\right) + 0.5\left(d_{i-1}^n.d_{i-1}^n\right)\right) \\ & -2\left(\delta\bar{d}_i^n.\delta\hat{d}_i^n\right)\left(\left(\delta\bar{d}_i^n.\delta\hat{d}_i^n\right) + \left(d_{i-1}^n.\delta\hat{d}_i^n\right)\right) \end{aligned} \tag{24b}$$

$$b_3 = \left(\delta\bar{d}_i^n.\delta\hat{d}_i^n\right)^2 - \left(\delta\hat{d}_i^n.\delta\hat{d}_i^n\right)\left(\delta\bar{d}_i^n.\delta\bar{d}_i^n\right) \tag{24c}$$

Inequality (23) shows that any arbitrary value is not acceptable for *FID*. This parameter should be provided in such a way that the inequality is satisfied. Putting the inequality (23) equal to zero, the roots are obtained as follows

$$\begin{cases} (FID_i^n)_{1,2} = \pm\sqrt{\dfrac{-b_2+\sqrt{\Delta}}{2b_1}} \\ (FID_i^n)_{3,4} = \pm\sqrt{\dfrac{-b_2-\sqrt{\Delta}}{2b_1}}, \qquad \Delta = \sqrt{{b_2}^2 - 4b_1b_3} \end{cases} \tag{25}$$

In each iteration of the loading step, the value of FID_i^n must satisfy Eq. (23). Otherwise, according to the roots of the equation and sign determination, an appropriate value for FID_i^n must be selected.

3.4 Convergence criteria

As described previously, FID_1^n can be fixed during loading of structure or changed in each loading step. Although in the present paper the first strategy is used, as for the second approach, it can be expressed that the value of FID_1^n can be changed according to the changes of structure stiffness. In fact, in the vicinity of limit points, it is better to use smaller amounts of FID_1^n. Meanwhile, when the behavior of structure is close to linear, it is possible to increase the value of FID_1^n. Moreover, in both approaches, in order to achieve convergence, the value of FID_i^n must be decreased in each iteration of load increment. In this paper, the term FID_i^n is reduced in each iteration as

$$FID_i^n = \alpha^{(i-1)} FID_1^n \tag{26}$$

In Eq. (26), α is constant coefficient $(0 < \alpha < 1)$. The authors proposed that $\alpha = 0.9$ will result in the best approximation. Value of FID_1^n parameter can be considered different for each problem. Here the author proposed 0.01 for this parameter.

In the present method, the relation below was proposed as the convergence criteria:

$$Error = \left|R_i^n\right| \;\le\; Tolerance = \frac{\left|R_1^n\right|}{\gamma} \tag{27}$$

Actually, the error is the length of unbalanced force vector calculated in each iteration of every increment. Convergence tolerance is defined as a fraction of the length of unbalanced force in the first iteration of each load increment. γ is a constant value greater than unity. The authors proposed that $5 \le \gamma \le 10$ is an appropriate range, so in the present study assumed $\gamma = 5$.

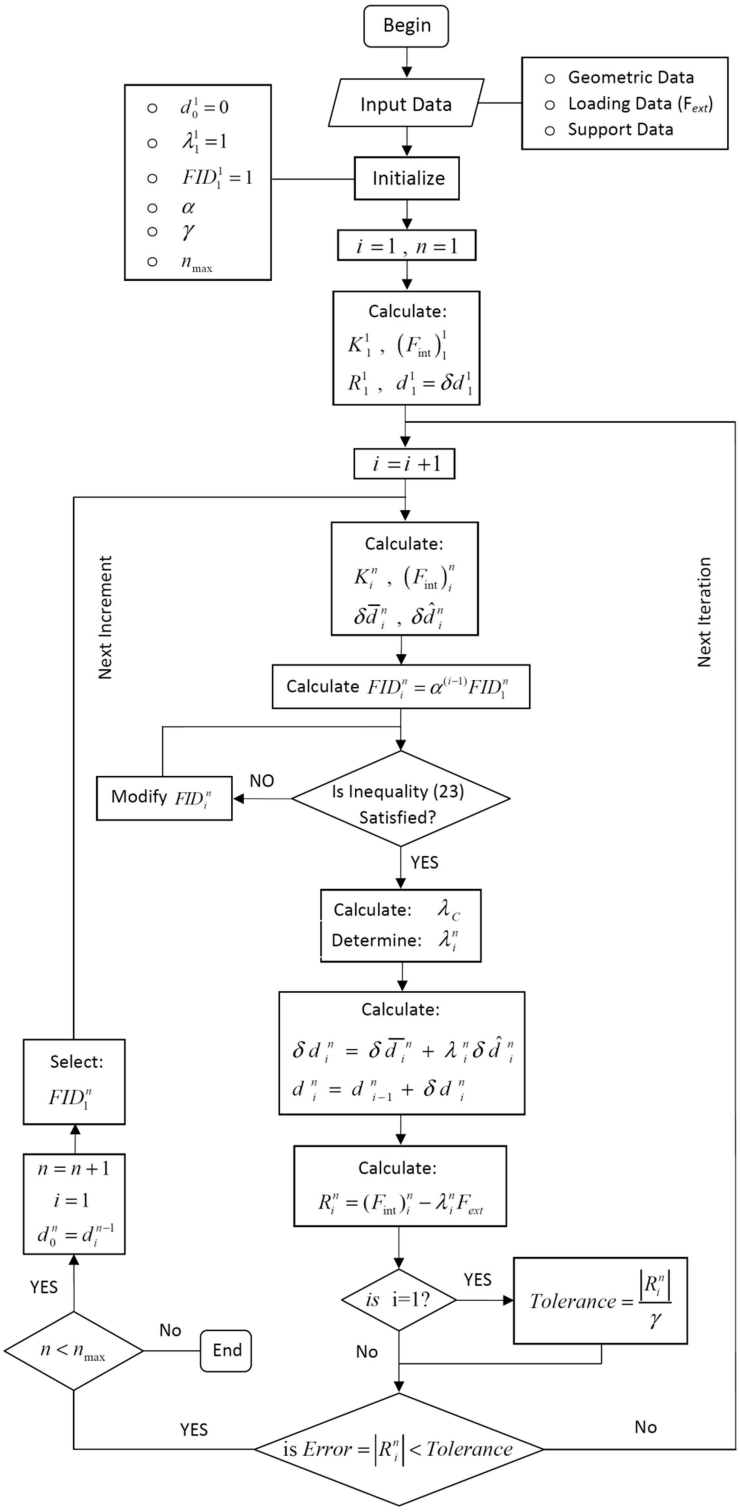

Figure 4. Flowchart of the FID algorithm

3.5 Nonlinear solution algorithm

A computer program based on proposed method has been written in MATLAB and representative results are provided. The *FID* algorithm can be described in a step-by-step procedure as follows:

Step 1: Initialize variables and parameters, such as structural geometry, connectivity, boundary conditions, and material properties.

Step 2: Determine the initial load factor λ_1^1, $\lambda_{\max}$, $n_{\max}$, α, γ and FID_1^n parameters.

Step 3: For the first iteration of the first load increment $(i=1, n=1)$, form tangent stiffness matrix and calculate internal force, unbalanced force and displacement vectors.

Step 4: For the load increments after the first step let $i=i+1$;

4-1: Calculate tangent stiffness matrix and internal force vector.

4-2: Calculate vectors $\delta\bar{d}_i^n$ and $\delta\hat{d}_i^n$ according to Eqs. (14) and (15).

4-3: Calculate FID_i^n according to Eq. (26).

4-4: Control inequality (23) and modify FID_i^n parameter to satisfy this inequality.

4-5: Calculate λ_c according to Eq. (20).

4-6: Determine appropriate load factor λ_i^n according to Eq. (16) and (21).

4-7: Calculate δd_i^n according to Eq. (13) and $d_i^n = d_{i-1}^n + \delta d_i^n$.

4-8: For $i=1$ calculate *Tolerance* value according to Eq. (27)

4-9: Calculate unbalanced force vector according to Eq. (10)

4-10: Calculate *Error* according to Eq. (27).

4-11: Return to the top of the fourth step until inequality (27) is satisfied.

Step 5: Check the termination: whether the total number of steps (increments, *n*) is smaller than the preset number $n_{\max}$ or whether the load factor λ_i^n at the end of increment is smaller than the allowable value $\lambda_{\max}$ let $n=n+1$ and $i=1$and go to step 4. Otherwise, stop the procedure. A flowchart of the above procedure is illustrated in Fig. 4.

4. NUMERICAL EVALUATIONS

In this section, the validity of the proposed method is confirmed by the examination of several results. Four examples are presented and discussed to verify the accuracy of the proposed procedure in predicting large deflection inelastic behavior of space steel trusses. For solving nonlinear equations, a new iterative method is adopted and the iterative process will stop when the convergence criteria is satisfied. Two cases of elastic analysis and inelastic post-buckling (IPB) analysis have been performed using the following properties: $\bar{X}_1=50$; $\bar{X}_2=100$; $\sigma_r=0.4\sigma_{cr}$. The computer program is developed based on the procedure described in this paper. The numerical examples were solved in a microcomputer environment so that the efficiency of the proposed procedure obtained from the present study can be compared with the modified arc-length method (cylindrical arc-length method) in nonlinear behavior of space

trusses. The cylindrical arc-length method is developed by Crisfield [24].

4.1 Toggle truss

The toggle truss described in Fig. 5 has been investigated by many researchers. The truss is composed of two identical members with the area of 96.77 cm^2 and moment of inertia of 745.18 cm^4. The elastic modulus and yield stress of the material are $E = 7.03 \times 10^5$ kg/cm^2 and $\sigma_y = 4 \times 10^4$ kg/cm^2, respectively. This truss analyzed previously by Papadrakakis [6], using the dynamic relaxation method for various stress-strain relationships, Hill et al. [9] using the arc-length method and also by Thai and Kim [32] using the GDC method.

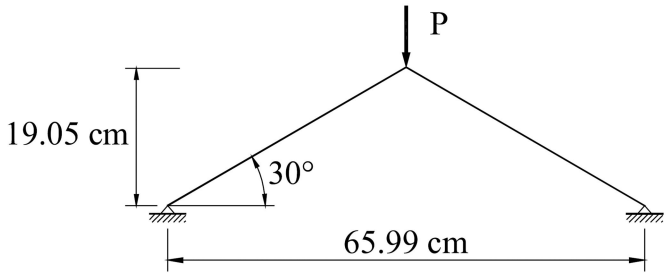

Figure 5. Toggle truss

Fig. 6 depicted the comparison of load-displacement curves obtained by the present study and arc-length method for elastic and IPB analysis. It is clear that the results of the proposed method are very close to those resulted from arc-length method. The limit loads obtained by the present work and arc-length method for elastic and IPB analysis are presented in Table 1. In this table we consider the results obtained from the arc-length method as reference solution. So the differences of limit loads predicted by present study using FID method and reference method are 1.309% and 1.034% for elastic and IPB analysis, respectively.

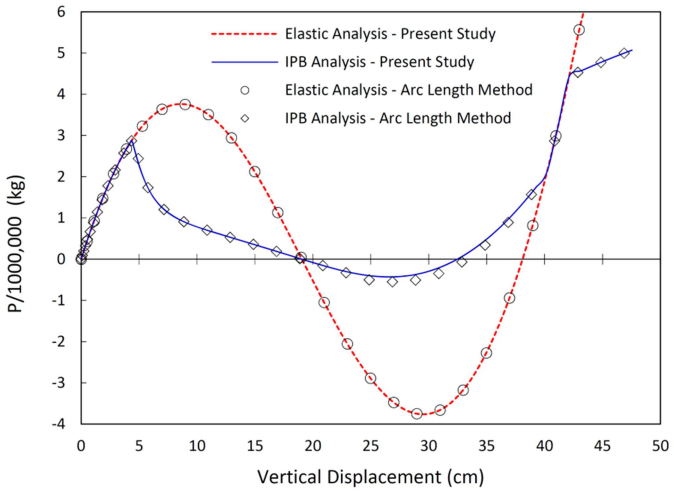

Figure 6. Load-displacement curve for toggle truss

Table 1:Analysis result of toggle truss

Analysis type	Limit load (kg)Arc-length	Present	Error (%)
Elastic	3.82×10^6	3.77×10^6	1.309
IPB	2.9×10^6	2.87×10^6	1.034

4.2 Star dome truss

Fig.7 shows configuration of a 24-member star dome truss subjected to an external concentrated load P at the center with its associated data. This structure has 21 degrees of freedom. all members of the truss has a cross-sectional area of 0.1 cm^2 and weak axis moment of inertia of 0.00417 cm^4. The elastic modulus and yield stress of the material are $E = 2.034\times10^7$ N/cm^2 and $\sigma_y = 4\times10^4$ kg/cm^2, respectively. This structure was analyzed previously by Hill et al. [9], Ramesh and Krishnamoorthy [15] and Thai and Kim [32] using the arc-length, the dynamic relaxation and GDC method respectively.

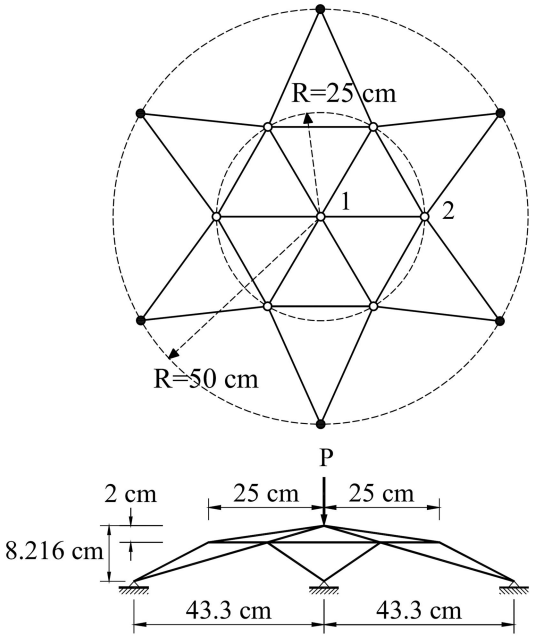

Figure 7. Star dome truss

This three dimensional truss has been analyzed using the method developed in this paper and the equilibrium path has been drawn as shown in Fig. 8. This figure illustrated the load-displacement curve of node 1 obtained by the present study and arc-length method for elastic and IPB analysis. It is observed that the result obtained by the proposed procedure are in good agreement with those resulted from the arc-length method. The equilibrium paths of the truss at node 2 for elastic and IPB analysis are also shown in Fig. 9. The limit loads obtained by the present work and arc-length method for elastic and IPB analysis are also presented in Table 2. The differences of limit loads predicted by present study and arc-

length method are 0.154% and 0.089% for elastic and IPB analysis, respectively.

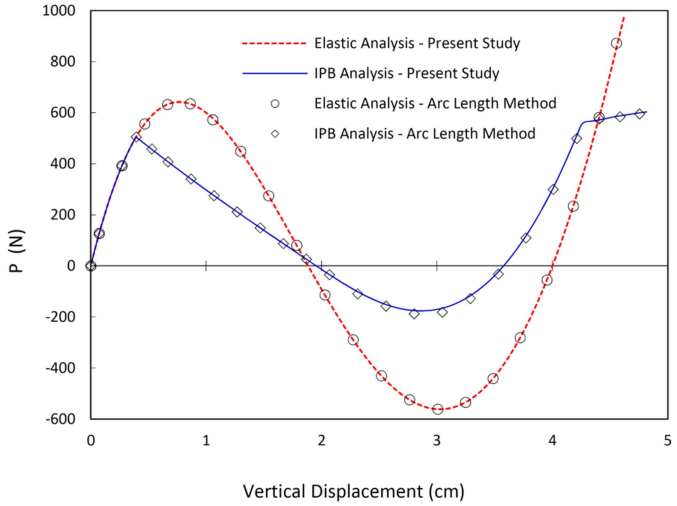

Figure 8. Load-displacement curves of star dome truss at node 1

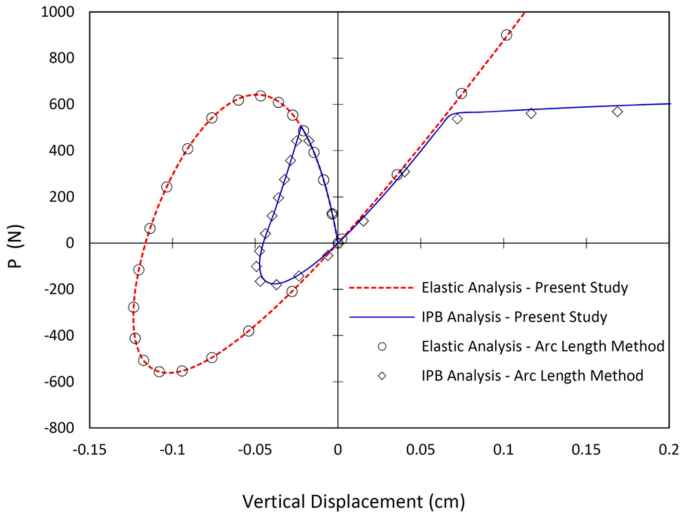

Figure 9. Load-displacement curves of star dome truss at node 2

Table 2: Analysis result of star truss

Analysis type	Limit load (kg)Arc-length	Present	Error (%)
Elastic	641.07	642.06	0.154
IPB	504.46	504.91	0.089

4.3 Geodesic dome truss

Configuration of the geodesic dome truss, composed of 156 members and 61 nodes, shown in Fig. 10 is taken from Ramesh *and* Krishnamoorthy [15]. This truss is subjected to concentrated vertical load at the center. All members have identical cross sections of 6.5 cm^2 and weak axis moment of inertia of 1.0 cm^4. The elastic modulus and yield stress of the

material are $E = 6895\ \text{KN/cm}^2$ and $\sigma_y = 400\ \text{KN/cm}^2$, respectively. The elevation of the truss is defined by the equation $x^2 + y^2 + (z + 7.2)^2 = 60.84$.

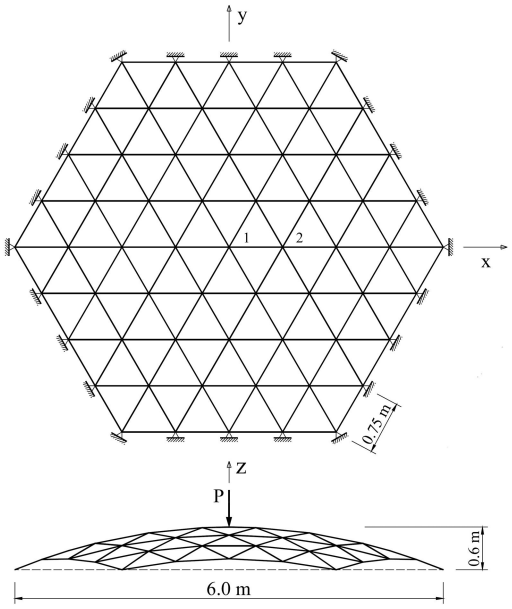

Figure 10. Geodesic dome truss

The load-displacement curve for node 1 and 2 of this structure is shown in Fig. 11 and Fig. 12, respectively. The comparison shows that the curves obtained by the present study are nearly coincident with the curves resulted from arc-length method for elastic and IPB analysis. The limit loads obtained by the present work and arc-length method for elastic and IPB analysis are also presented in Table 3. The differences of limit loads predicted by present study and arc-length method are 0.635% and 0.766% for elastic and IPB analysis, respectively.

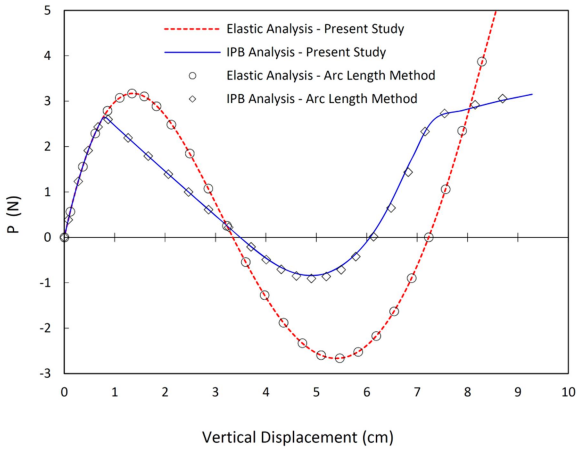

Figure 11. Load-displacement curve for geodesic dome truss at node 1

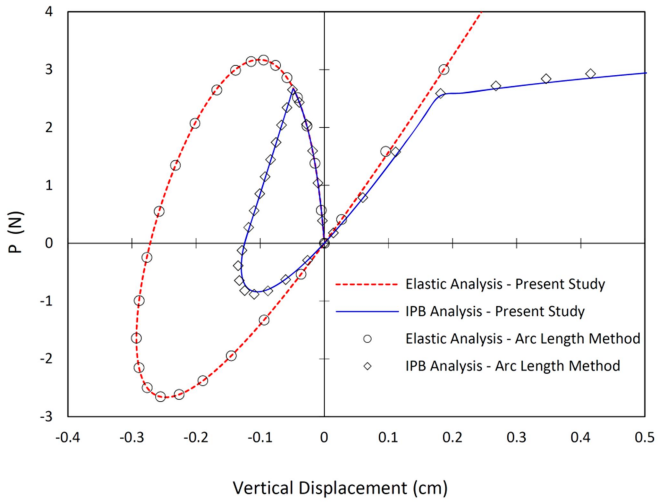

Figure 12. Load-displacement curve for geodesic dome truss at node 2

Table 3:Analysis result of star truss

Analysis type	Limit load (kN)Arc-length	Present	Error (%)
Elastic	3.15	3.17	0.635
IPB	2.61	2.63	0.766

4.4 Two-dimensional circular arch truss

Fig. 13 shows a two-dimensional circular arch truss, composed of 101 elements, taken from Crisfield [36]. This structure was analyzed by Hrinda [37] using the arc-length method and Thai and Kim [32] using the GDC method. This truss is subjected to a vertical load of 4 *MN* at the apex. All members of the truss are assumed to have the same cross-sections with $EA = 50MN$.

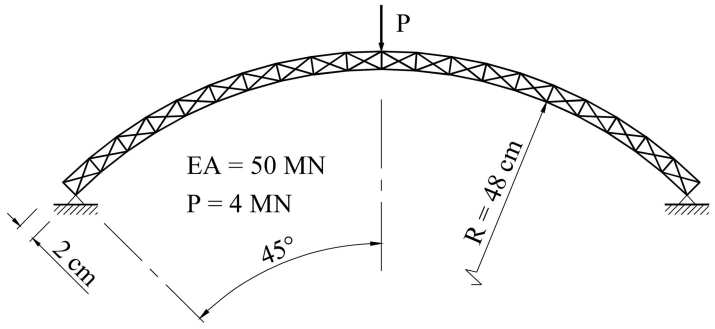

Figure 13. A two-dimensional circular arch truss

The equilibrium path curves of this truss for elastic analysis obtained by the present method and arc-length method are compared in Fig. 14. It can be seen that the results generated by the present study are almost identical with those predicted by the arc-length

method. The snap-back and snap-through points resulted from the present study occur at the same point obtained from the arc-length method. This example demonstrates the efficiency and capability of the proposed method in tracing the equilibrium path of highly nonlinear trusses involving complex snap-through and snap-back phenomena.

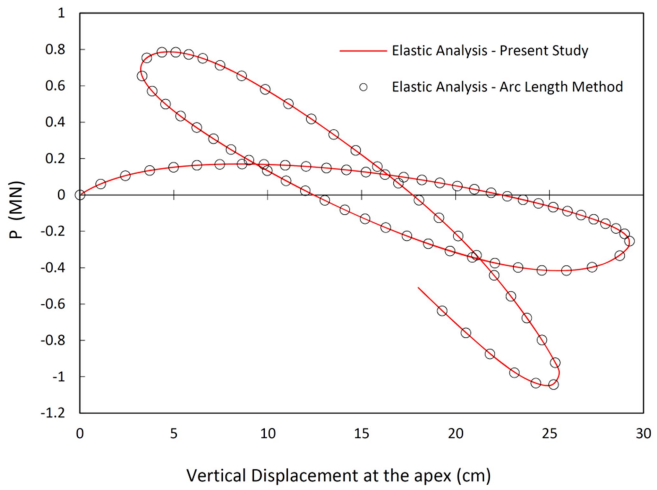

Figure 14. Load-displacement curves of two-dimensional circular arch truss

5. CONCLUSIONS

In this paper, a new scheme was proposed for large deformation inelastic post-buckling analysis of space truss structures. An incremental-iterative procedure was derived, based upon the displacement control scheme, using fixed incremental displacement (FID). By employing a specified displacement, the corresponding load will be obtained. In the present method the ratio of the size of increment displacement vector to that of total displacement is assumed to be constant at the beginning of each increment. A numerical procedure has been developed and implemented into a computer program. Numerical examples demonstrate the feasibility and accuracy of the FID algorithm, to be highly suitable in predicting nonlinear response of structures with multiple limit points and snap-back points, and trace the equilibrium path accurately. In spite of the fact that the procedure herein explained is only implemented for truss structures, it is possible to generate the proposed method for other structures.

REFERENCES

1. Turner MJ, Dill EH, Martin HC, Melosh RJ. Large deflection of structures subject to heating and external load, *Journal of Aerosol Science*, **27**(1960) 97-106.
2. Argyris JH. *Recent Advances in Matrix Methods of Structural Analysis*, Pergamum Press, Oxford, 1964.

3. Marcal PV. Finite element analysis of combined problems of material and geometric behavior, *Proceeding of American Society of Mechanical Engineering, Conference on Computational Approaches in Applied Mechanics*, June 1969.
4. Zienkiewicz 0C. *The Finite Element in Engineering Science*, McGraw-Hill, London, 1971.
5. Yamada Y, Yoshimura N, Sakurai T. Plastic stress-strain matrix and its application for the solution of elasto-plastic problems by the finite element method*, International Journal of Mechanical Sciences*, **10**(1968) 343-54.
6. Papadrakakis M. Inelastic post-buckling analysis of trusses, *Journal of Structural Engineering*, **109**(1983) 2129-47.
7. Smith E. Space truss nonlinear analysis, *Journal of Structural Engineering,* **110**(1984) 688-705.
8. Murtha-Smith E. Alternate path analysis of space trusses for progressive collapse, *Journal of Structural Engineering*, **114**(1988) 1978-99.
9. Hill CD, Blandford GE, Wang ST. Post-buckling analysis of steel space trusses, *Journal of Structural Engineering*, **115**(1989) 900-19.
10. deFreitas JAT, Ribei ACB. Large displacement elasto-plastic analysis of space trusses,*Computers & Structures*, **44**(1992) 1007-16.
11. Murtha-Smith E. Compression-member models for space trusses: Review, *Journal of Structural Engineering*, **120**(1994) 2399-2407.
12. Blandford G. Review of progressive failure analysis for truss structures, *Journal of Structural Engineering*, **123**(1997) 122-9.
13. Blandford G. Large deformation analysis of inelastic space truss structures, *Journal of Structural Engineering*, **122**(1996) 407-15.
14. Blandford G. Progressive failure analysis of inelastic space truss structures, *Journal of Structural Engineering*, **58**(1996) 981-90.
15. Ramesh G, Krishnamoorthy CS. Inelastic post-buckling analysis of truss structures by dynamic relaxation method, *International Journal for Numerical Methods in Engineering*, **37**(1994) 3633-57.
16. Jagannathan DS, Christiano P, Epstein HI. Nonlinear analysis of reticulated space trusses, *ASCE, Journal of the Structural Division*, **101**(1975) 2641-58.
17. Toklu YC. Nonlinear analysis of trusses through energy minimization, *Computers & Structures*, **82**(2004) 1581-9.
18. Saffari H, Mansouri I. Non-linear analysis of structures using two-point method, *International Journal of Non-Linear Mechanics*, **46**(2011) 834-40.
19. Saffari H, Shojaee S, Rostami S, Malekinejad M. Application of cubic spline on large deformation analysis of structures, *International Journal of Steel Structures,***14**(2014) 165-72.
20. Brebbia C, Connor J. Geometrically non-linear finite element analysis, *Journal of the Engineering Mechanics Division*, **95**(1969) 463-83.
21. Murray DW, Wilson EL. Finite element post-buckling analysis of thin elastic plates, *Journal of the Engineering Mechanics Division*, **9**(1969) 143-65.
22. Oden JT. Numerical formulation of non-linear elasticity problems. *ASCE, Journal of the Structural Division*, **93**(1967) 235-55.
23. Oden JT. Finite element applications in non-linear structural analysis, *Proceeding*

Conference on Finite Element Method, Vanderbilt University, Tennessee, November 1969.
24. Crisfield MA. *Non-Linear Finite Element Analysis of Solids and Structures*, Essential, John Wiley, New York, Vol. 1, 1991.
25. Chan SL, Chui PPT. *Non-Linear Static and Cyclic Analysis of Steel Frames with Semi-Rigid Connections*, Elsevier Science, Netherlands, 2000.
26. Eriksson A. Derivatives of tangential stiffness matrices for equilibrium path predictions, *International Journal for Numerical Methods in Engineering*, **2**(1991) 1093-1113.
27. Kwasniewski L. Complete equilibrium paths for Mises trusses, *International Journal of Non-Linear Mechanics*, **44**(2009) 19-26.
28. Riks E. The application of Newton's method to the problem of elastic stability, *International Journal of Applied Mechanics*, **39**(1972) 1060-5.
29. Riks E. An increment approach to the solution of snapping and buckling problems, *International Journal of Solids and Structures*, **15**(1979) 529-51.
30. Crisfield MAA. Fast incremental/iterative solution procedure that handles 'snap-through', *Computers and Structures*, **13**(1981) 55-62.
31. Saffari H, Fadaee MJ, Tabatabaei R. Nonlinear analysis of space trusses using modified normal flow algorithm, *Journal of Structural Engineering*, **134**(2008) 998-1005.
32. Thai HT, Kim SE. Large deflection inelastic analysis of space trusses using generalized displacement control method, *Journal of Constructional Steel Research*, **65**(2009) 1987-94.
33. Saffari H, Mirzai NM, Mansouri I. Bagheripour MH. Efficient numerical method in second-order inelastic analysis of space trusses, *Journal of Computing in Civil Engineering*, **27**(2013) 2129-38.
34. Kassimali A, Bidhendi E. Stability of trusses under dynamic loads, *Computers and Structures,* **29**(1988) 381-92.
35. Tezcan SS. Discussion of numerical solution of non-linear structures, by Poskitt TJ, *Journal of the Structural Division*, *ASCE,* **94**(1968) 1613-23.
36. Crisfield MA. *Non-Linear Finite Element Analysis of Solids and Structures*, Advanced topics, John Wiley, New York, Vol. 2, 1997.
37. Hrinda GA. Geometrically nonlinear static analysis of 3D trusses using the arc-length method, *WIT Transactions on Modelling and Simulation*, **46**(2007) 243-52.